PROCEEDINGS OF SPIE

Plasma optics for intense laser amplification

Kenan Qu, Nathaniel J. Fisch

SPIE.

Plasma optics for intense laser amplification

Kenan Qu and Nathaniel J. Fisch

Department of Astrophysical Sciences, Princeton University, Princeton, New Jersey 08544, USA

March 5, 2019

ABSTRACT

Laser amplification through plasma-based techniques might overcome the thermal damage limit of conventional materials, thereby enabling the next generation of laser intensities. The leading plasma-based method is Raman compression: a long laser pump decays into a plasma wave and a counterpropagating short laser seed pulse, which, capturing the pump energy, reaches extreme intensities. The technological requirements on the seed are severe: it must be very sharp and matched properly in frequency. To sharpen the seed pulse, we propose a laser-controlled, super-fast plasma shutter technique, analogous to electromagnetically induced transparency (EIT) in atoms. We further show that the laser seed may even be replaced by a stationary plasma wave seed. In the important pump-depletion regime, the plasma-wave initiated output pulse approaches the self-similar attractor solution for the corresponding laser seed, with the frequency match automatic. These techniques also work with partially coherent pumps. Actually, a partially coherent pump can even advantageously suppress the noise-seeded spontaneous Raman amplification which is responsible for premature pump depletion.

Keywords: Plasma Raman amplification, Intense laser pulse, electromagnetically induced transparency, Langmuir wave, laser coherence

1. INTRODUCTION

Contemporary technologies of processing and manipulating lasers are developed based on solid-state materials,. They include filters, diffusers, polarizers, gratings, holograms plates, and a myriad of different nonlinear optical crystals. These solid-state optical elements are susceptible to thermal damage[1,2] at high laser intensities or high laser pulse energies. Hence, high energy density applications often require large-scale special-made optical elements[3] and splitting an energetic laser pulse into multiple beams for processing before merging them at the end.[4] In recent years, plasma optics has been exploited to solve the issues related to optically induced damage by taking advantage of the damage-less feature of the plasma medium. Different plasma optical elements have been proposed including laser intensity amplification,[5–7] pulse compression,[6] wavefront sharpening,[8] beam combining,[9] coherence cleaning,[10] polarization[11–13] and optical vortex manipulation,[14–18] plasma grating,[19] plasma photonic crystals,[20–22] plasma holography,[17,23] and frequency conversion.[24,25]

In particular, backward Raman amplification[5,6,26–31] promises to deliver multipetta-watt laser intensity using centimeter-diameter plasmas. In a plasma Raman amplifier, a long pump laser pulse with frequency ω_0 and wavenumber k_0 is sent into plasma characterized by the plasma frequency ω_p, shown as in Fig. 1(a). A counter-propagating seed pulse with frequency $\omega_0 - \omega_p$ begins to interact with the pump at the exit boundary of the plasma. Mediated by an active plasma wave, the energy quickly flows from the high-frequency pump into the low-frequency seed at a large interaction rate $\gamma = (a_0/2)\sqrt{\omega_0\omega_p}$ where $a_0 = 8.55 \times 10^{-10}\sqrt{I_0\lambda^2(\mathrm{W\,cm^{-2}\mu m^2})}$ is the dimensionless pump amplitude, I_0 is the intensity, and λ is the wavelength. For example of a $0.8\,\mu\mathrm{m}$ pump laser with intensity $1 \times 10^{15}\,\mathrm{W\,cm^{-2}}$ and plasma with $\omega_p = \omega_0/10$, the characteristic length for pump energy transfer is only $c/\gamma \approx 20\,\mu\mathrm{m}$. Thus, a moderate-intensity seed can quickly deplete the pump. The counter-propagating configuration allows the pump energy to accumulate at the front of the seed pulse in the pump-depletion regime, which effectively compresses the long pump pulse into a short and ultra-intense pump, as shown in Fig. 1(b). It can achieve nearly complete photon number conversion and the energy conversion efficiency is limited only by the ratio $(\omega_0 - \omega_p)/\omega_0 \approx 90\%$.[6] This mechanism is expected to lead to output at $10^{17} - 10^{18}\,\mathrm{W\,cm^{-2}}$ intensity and petawatt pulse power using centimeter-long plasma.[26,27]

Figure 1. (a) Backward Raman amplification using a long pump pulse and a short seed pulse in plasma. (b) In the case of an advantageous result, the amplified output pulse assumes a π-pulse shape accompanied by depletion of the pump laser.

Experimental implementations of the promising ultra-intense light source have been carried out in multiple facilities.[28–40] Remarkably high amplification rate compared with traditional solid-state lasers has been reported in an only $4-$mm long plasma[31,34] to produce $2.5 \times 10^{16}\,\mathrm{W\,cm^{-2}}$ intensity, which is over two orders of magnitude higher than the pump. Further improving the experimental performance requires overcoming the limiting factors[41] and one of the most stringent requirements is the quality of the seed pulse. In backward Raman amplification, the advantageous pump-depletion stage happens only following a linear stage when the seed intensity is much lower than the pump intensity. In the linear stage, the seed grows exponentially at the growth rate of 2γ and the pump intensity remains a constant. Although the seed has the largest growth rate in this stage, the pump energy is not efficiently captured by the seed pulse. The preferable nonlinear pump-depletion stage begins when the seed intensity is similar to the pump intensity. At this stage, the ponderomotive force from the beat of pump and seed pulses excite large-amplitude plasma Langmuir waves. The pump energy is strongly back-scattered by the plasma wave into the seed pulse. For sufficiently strong seed, the full pump energy can be converted into seed pulse energy and plasma waves.

An ideal seed pulse has a δ-function shape envelope for its high peak intensity and sharp wavefront. Upon interaction with the pump beam, it immediately begins to capture all the energy of the pump beam. The seed pulse energy can be converted back into the pump by combining with the plasma wave. The nonlinear interplay of the three waves results in a wave train, called the "π-pulse" solution. The peak amplitude of the π pulse is determined by the seed capacity ϵ which is defined as the integrated amplitude of the initial seed. A larges seed capacity ϵ (despite it generally being a small number) yields a higher energy concentration to the leading spike in the π pulse train and hence a higher peak intensity. When $\epsilon > 0.1$, the main peak contains over 50% of the total pulse energy. The peak intensity of the amplified pulse can be further increased by operating at the Langmuir wave-breaking regime[42,43]—the plasma wave exceeds its threshold amplitude and quickly decays—to prevent the energy scattering from the seed to pump. At this limit, the compression efficiency can reach nearly 100%.

For non-ideal seeds, it is important to have a sharp wavefront without pedestals. Such a seed gets amplified first through the linear stage and reach the pump intensity before its duration contracts. However, any pre-pulses would also quickly grow due to the high linear growth rate, and would compete with the main seed pulse to cause premature pump energy spread.[44] A finite seed duration[45] causes a reduction of the effective seed capacity because the weak seed front or pre-pulses shadows the rear layer of seed.

Providing the suitable seed laser pulse is difficult in experiments[35] because there is no pulsed laser available at the exact frequency $\omega_0 - \omega_p$. Currently, the majority of the experiments[29–38] create seed pulses by splitting a small portion of the pump energy and downshifting its frequency. The frequency downshift is achieved using optical parametric processes,[30,32] a Raman gas chamber,[33,35] a Raman crystal,[31,34,36,38] Raman scattering from a thick foil,[37] or block the high frequency components after spectrum broadening.[29] Since the frequency downconverters have poor energy conversion efficiency of up to 5%, the obtained seed pulses typically have low seed capacities even after compression. Only a few exceptions of the reported experiments[28,39,40] were able to use a separate laser to serve the seed pulse, but the burden is put onto fine tuning the plasma density to ensure the frequency match.

Less addressed in the experiments is the contrast ratio of laser pulses[46] which crucially determines the efficiency of backward Raman amplification.[26,44,45,47,48] The pulse contrast ratio quantifies the wavefront sharpness using the ratio of laser pulse peak intensity to pre-pulse or pedestal intensity. For all the above-mentioned methods of seed pulse generation,[28–40] the pulse contrast ratio is fundamentally limited by the pulsed laser or the

chirped pulse amplification system. In the time frame of several nanoseconds,[49, 50] pre-pulses are generated by the neighboring pulses from the oscillator or regenerative laser cavities. For sub-nanosecond pulses,[50, 51] they are accompanied by a nanosecond pedestal which results from the amplification of spontaneous emission (ASE),[51] *i.e.,* amplified fluorescence in the pump crystal. Pulses with picosecond durations usually suffer from degradation close to the peak intensity due to deficient laser spectra and imperfect pulse compression.[52] Contrast ratio of femtosecond pulse lasers[53] are challenged by the management of different optical nonlinearities and residual high-order dispersion.

The Raman instability of pre-pulses and pulse pedestals limits the amplification performance.[26, 27, 44] To suppress the parasitic Raman instability, theoretical analysis[26, 27, 44] was focused on using chirped pump beam and plasma density gradient. When the chirped pump beam transverses through the plasma with a changing density, the frequency matching condition is satisfied only at a single location and, by careful arrangement, this location travels at the group velocity of the seed pulse. Provided that the slope of chirping is large, the Raman growth rate outside the location is greatly limited by detuning. Unwanted Raman instabilities are suppressed making it robust to noise. The main seed pulse, due to its broad spectrum, can tolerate random fluctuation of the plasma density. However, the setup needs precisely controlled laser chirping and plasma density gradient which makes difficult experimental demonstration.

To solve these issues related to preparing seeds for backward Raman amplification and suppressing the unwanted noise amplification, three methods[7, 8, 10] are proposed using plasma optics techniques. The first method is to design a plasma-based optical shutter[8] for creating a sharp wavefront in a laser pulse while maintaining or even amplifying its intensity. The mechanism of the optical shutter is analogous to the electromagnetically induced transparency in atoms: the interference of the probe beam and the control-probe-plasma three wave interaction induces a transparency window below the plasma "cut-off" frequency only when the control laser intensity exceeds a certain threshold. It transforms the gradual variation of optical intensity into an abrupt transmittance, thereby creating a sharp wavefront to the seed beam.

The second method completely avoids any complication of preparing a laser seed by replacing it with a plasma wave seed[7] . We prove that a plasma wave seed may be found by construction that strictly produces the same output pulse as does a counter-propagating laser seed at least in the regime in which the amplification is most efficient. In the nonlinear regime, or pump-depletion regime, the plasma-wave-initiated output pulse approaches the same self-similar attractor solution for the corresponding laser seed. In addition, chirping the plasma wave wavelength can produce the same beneficial effects as chirping the seed wave frequency. This methodology is attractive because it avoids issues in preparing and synchronizing a frequency-shifted laser seed.

The third method uses a partial coherent pump laser,[10] instead of a fully coherent pump laser, to suppress the amplification of unwanted noise signals. We show that a finite correlation length of the pump leads to a reduction of the linear Raman growth rate but it does not affect the pump depletion in the nonlinear regime. The incoherence on scales shorter than the instability growth time suppresses spontaneous amplification of noise, thereby partially coherent lasers can serve as efficient low-noise Raman amplification pumps.

This paper reviews the theoretical progress in addressing the issues relating to the seed and noise in backward Raman amplifications using these three plasma optics techniques. The details of the paper are outlined as follows: In Sec. 2, we present the optical shutter based on electromagnetically induced transparency to create a sharp wavefront to a laser pulse for seeding the backward Raman amplification. In Sec. 3, we explain how a plasma wave seed can replace the laser seed to trigger Raman amplification and obtain the same self-similar attractor solution. In Sec. 4, we present a theory for suppressing the noise induced amplification by optimizing the correlation length of the pump beam. In Sec. 5, we summarize out results.

2. SHARP SEED WITH ELECTROMAGNETICALLY INDUCED TRANSPARENCY

The proposed optical shutter[8] comprises of a high-density plasma slab and a moderate-intensity control laser beam, as shown in Fig. 2. It sharpens a weak seed pulse that is generated either by a separate laser or by splitting a small portion of the control laser energy and downshifting its frequency. The plasma slab blocks the propagation of the seed laser that is below the "cut-off" frequency. However, the plasma slab becomes transparent when irradiated by a control laser beam through EIT[8, 54–59]—the control laser above threshold intensity can induce a

transparency window in the plasma slab for a seed laser that is below the "cut-off" frequency. For nonrelativistic laser beams, the plasma slab, functioning as a superfast optical shutter, only abruptly lets the seed laser transmit when the control beam intensity exceeds a threshold value. This abruptness creates a sharp wavefront in the seed transmission. Unlike relativistic transparency,[60] EIT arises from interference within the plasma wave interacting with different laser fields, in comparison to relativistic transparency which drives electrons near the speed of light. This allows the use of weak control beam lasers whose intensity can be well below the relativistic regime, *e.g.* a few $PW\,cm^{-2}$. More importantly, the control pulse can also amplify the seed through an instability yielding a strong and sharp pulse for seeding backward Raman amplification.
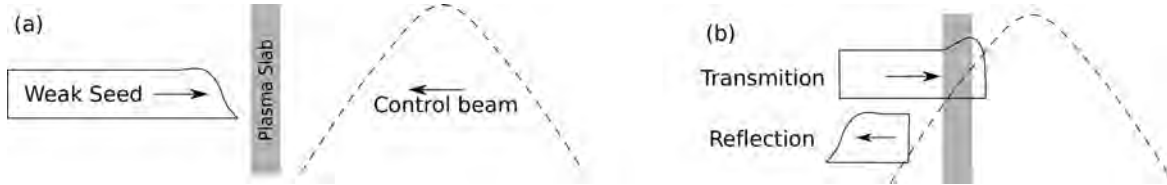

Figure 2. Schematics of the optical shutter using two broad pulses with a high-density plasma slab. (a) A nonsharpened seed below the plasma "cut-off" frequency gets constantly reflected in absence of control beam in plasma slab. (b) When the control beam intensity exceeds the threshold value, the seed is abruptly let through creating a sharp wavefront. Adapted from *Qu and Fisch (2017)*,[8] with the permission of AIP Publishing.

The transmittance of the optical shutter is analyzed using the dispersion relation. Interaction of the laser beams in the plasma can be modeled with the conventional three-wave equations[53]

$$(\partial_{tt} - c^2\partial_{zz} + \omega_p^2)\boldsymbol{A}_0 = -\omega_p^2\frac{n}{\bar{n}}\boldsymbol{A}_1, \tag{1}$$

$$(\partial_{tt} - c^2\partial_{zz} + \omega_p^2)\boldsymbol{A}_1 = -\omega_p^2\frac{n}{\bar{n}}\boldsymbol{A}_0, \tag{2}$$

$$(\partial_{tt} + \omega_p^2)n = \bar{n}c^2\partial_{zz}(\boldsymbol{A}_0 \cdot \boldsymbol{A}_1), \tag{3}$$

where $\boldsymbol{A}_0$ and $\boldsymbol{A}_1$ are the vector potentials of the control beam and the seed beam normalized to $e/m_e c$, respectively, $\bar{n}$ is the unperturbed electron density, n is the perturbed electron density, and $\omega_p = \sqrt{\bar{n}e^2/\epsilon_0 m_e}$. Here e is the natural charge; m_e is the electron mass; c is the speed of light; and ε_0 is the permittivity of free space. For non-depleted control beam, the dispersion relation is found in the frequency regime

$$\omega_1^2 - c^2\boldsymbol{k}_1^2 = \omega_p^2 - fc^2(\boldsymbol{k}_0 - \boldsymbol{k}_1)^2, \tag{4}$$

$$f = A_0^2/[1 - (\Delta\omega/\omega_p)^2], \tag{5}$$

where $\Delta\omega = \omega_0 - \omega_1$ is the two-photon detuning. Compared with the normal dispersion relation of electromagnetic waves in plasma, Eq. (4) includes an extra term which depends on the intensity of the control beam if $\Delta\omega \neq \omega_p$. This term captures the plasma wave generated by the ponderomotive force of the seed-control beat. The conditions of induced transparency can then be found as

$$\left|\boldsymbol{k}_1 - \frac{f}{1-f}\boldsymbol{k}_0\right| = \frac{1}{(1-f)c}\sqrt{f(\omega_0^2 - \omega_1^2) - (\omega_p^2 - \omega_1^2)}. \tag{6}$$

The threshold intensity of the control beam for EIT is

$$A_0^2 \geq A_{\mathrm{th}}^2 \equiv \left[1 - \left(\frac{\Delta\omega}{\omega_p}\right)^2\right]\frac{\omega_p^2 - \omega_1^2}{\omega_0^2 - \omega_1^2} \tag{7}$$

on the condition that $\omega_p > \Delta\omega > 0$; otherwise the inequality (7) is to be reversed.

We note that the threshold value for EIT [Eq. (7)] is independent of the directions of wavevectors, which allows to use an arbitrary angle between the control and seed beams. Although we focus on two counter-propagating lasers for simplicity of analysis and simulation, the flexibility might be an advantage in experiments as it avoids the issue of aligning two optical pulses.

As the seed beam propagates in the transparency window, it grows due to a parametric instability. The growth rate under the condition $\omega_0 \lesssim 2\omega_p$ can be approximated as

$$\Gamma_{\text{EIT}} = \frac{1}{2}\sqrt{A_0^2 \frac{2\omega_p^2(\omega_0^2 - \omega_p^2)}{\omega_0 \omega_h} - (\omega_p - \omega_0 + \omega_h)^2}, \tag{8}$$

where $\omega_h = \sqrt{\omega_p^2 + c^2 k_1^2}$. This instability is similar to the Raman instability but they are different. This can be seen from the frequency relations; EIT uses a nonresonant control beam $\omega_0 < \omega_1 + \omega_p$ and Raman instability requires a resonant control beam for the maximum growth rate. Actually, Raman instability does not exist in a plasma of above one quarter of the critical density, where EIT is operated. The seed wavefront continues to grow due to the instability and gets sharpened.

The seed wavefront sharpness, defined by the "rising-time" t_r, approaches the asymptotic value which is limited by the finite frequency bandwidth of the EIT window

$$t_r = \frac{1}{\omega_{\text{EIT}}} = \frac{1}{2\omega_p - \omega_0}. \tag{9}$$

For the maximum seed sharpness, the plasma frequency ω_p is preferably set close to half the control beam frequency ω_0. In the most favorable regime with seed frequency $\omega_1 \sim \omega_0/2$, the rising edge of the obtained pulse only contains a small number of optical cycles, i.e., $\omega_1 t_r \approx 1/[2(\omega_p/\omega_1 - 1)]$. Note that the input seed beam can be of any sharpness and even a continuous wave. Given a long plasma, the seed intensity can continue to grow. However, the seed also suffers strong group velocity dispersion (GVD) associated with the nonlinear dispersion relation whi ch reduces pulse sharpness. Thus, a thin plasma slab is desirable for optimal sharpness of the pulse output. Its minimum thickness is confined by seed tunneling with a characteristic length $c/\sqrt{\omega_p^2 - \omega_1^2}$. For higher pulse fluence, the sharpened pulse can be sent into a lower-density plasma medium for second stage amplification.

The "proof-of-principle" demonstration using full one-dimensional PIC simulation code EPOCH[61] is reported in Ref.[8] Two counter-propagating laser pulses are sent into a thin plasma slab which has a maximum density of $1.14 \times 10^{20}\,\text{cm}^{-3}$. The plasma slab is opaque for the seed until the control beam intensity exceeds the threshold intensity. The optical shutter produces a sharpened and amplified seed pulse with its rising time is reduced from $0.59\,\text{ps}$ to $0.1\,\text{ps}$ and its intensity increased by a factor of 8.
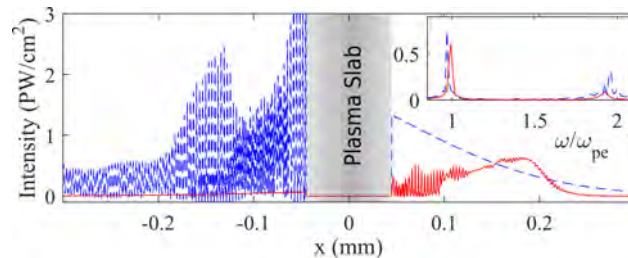

Figure 3. PIC simulation results of the laser pulses whose rising time is reduced from $0.59\,\text{ps}$ to $0.1\,\text{ps}$ and its peak intensity increased from $0.1\,\text{PW/cm}^2$ to $0.8\,\text{PW/cm}^2$. The plasma density has a Gaussian profile $n_e = 1.14 \times 10^{20} \times e^{-(x/30\mu\text{m})^2}\,\text{cm}^{-3}$. Adapted from *Qu and Fisch (2017)*,[8] with the permission of AIP Publishing.

As an application of the optical shutter, consider creating a sharp wavefront with a rising time of $t_r = 15\,\text{fs}$ on a broad laser pulse at $\lambda_1 = 0.8\,\mu\text{m}$ wavelength for seeding backward Raman amplification. The optimal wavelength of the control beam is then $\lambda_0 = \lambda_1/2 = 0.4\,\mu\text{m}$. To achieve the specific rising time, the frequency ratio of control beam and plasma is $\omega_0/\omega_p = 2/[1 + 1/(\omega_0 t_r)] \approx 1.97$. Using Eq. (7), we find the threshold value for the control beam $A_{\text{th}} \approx 0.017$, corresponding to $I_{\text{th}} \approx 2.5 \times 10^{15}\,\text{W cm}^2$. The density of the plasma slab should reach the density of $5.6 \times 10^{22}\,\text{cm}^{-3}$ and the minimum thickness of near $0.8\,\mu\text{m}$ to prevent tunneling.

3. RAMAN AMPLIFICATION WITH A PLASMA WAVE SEED

Stimulated Raman scattering can be excited with either a frequency-downshifted laser beam or a plasma Langmuir wave.[62] Compared with using a laser seed, using a plasma wave seed in backward Raman amplification could have engineering benefits. First, the plasma wave has a negligible group velocity, so without regard for synchronization, it can trigger backward Raman amplification only when the pump beam reaches it. Second, using a plasma wave seed also avoids the technological challenges of creating the exact frequency downshift. Third, a plasma wave seed can be created locally without pre-pulses or pedestals which are difficult to eliminate from ultrashort laser pulses.

To initiate powerful backward Raman amplification, the most important criterion is whether the plasma wave seed can yield the promising π-pulse solution of amplification—the pump pulse energy is consumed by a counter-propagating probe pulse that has a growing amplitude and a contracting duration. In Ref.,[7] such a plasma wave seed is constructed, through an equivalence condition between laser and plasma seeds, such that the amplified pulse will transition to the same nonlinear asymptotic attractor solutions which feature pump depletion. Under the equivalence condition, the envelopes of the plasma wave seed and the laser seed in the pump propagation direction z is related by

$$f_0(z) = \frac{c}{\gamma} \frac{\partial}{\partial z} b_0(z), \tag{10}$$

where b_0 and f_0 are the amplitudes of the laser seed and plasma wave seed. They are normalized by $b_0 = 8.55 \times 10^{-10} \sqrt{I_b \lambda^2 (\mathrm{W\,cm^{-2}\mu m^2})}$ and $f_0 = (e/m_e cV)|E_e|$, respectively, where $V \approx \sqrt{\omega_a \omega_p}/2$ for underdense plasmas (i.e., $\omega_a \approx \omega_b \gg \omega_p$ with ω_b being probe wave frequency) and linearly polarized optical beams. A plasma wave seed f_0 and a laser seed b_0, upon interaction with the same pump laser pulse, will generate probe pulse with asymptotically identical wavefronts, i.e.,

$$b_{\mathrm{f}}(t, z) = \int \mathrm{d}z' G_{\mathrm{bf}} f(t, z - z') \frac{c}{\gamma} \frac{\partial}{\partial z'} b_0(z') \cong \int \mathrm{d}z' G_{\mathrm{bb}}(t, z - z') b_0(z'), \tag{11}$$

where

$$G_{\mathrm{bf}}(t, z) = \frac{\gamma}{c} I_0(\xi) \cdot \Theta(t - \frac{z}{c}), \tag{12}$$

$$G_{\mathrm{bb}}(t, z) = \frac{1}{\gamma} \frac{\partial}{\partial t} G_{\mathrm{bf}}(t, z) = \frac{\gamma}{c} \sqrt{\frac{z}{ct - z}} I_1(\xi) \cdot \Theta(t - \frac{z}{c}) + \frac{1}{c} \delta(t - \frac{z}{c}), \tag{13}$$

are the Green's functions associated with the corresponding seeds.[63] Here $I_0(\cdot)$ is the zeroth order modified Bessel function, $\Theta(\cdot)$ is the Heaviside function, $\gamma = a_0 V$ denotes the linear temporal growth rate, and $\xi = 2(\gamma/c)\sqrt{z(ct - z)}$.

As the probe pulse propagates and grows, if initially short enough, it should eventually deplete the pump and enter into the nonlinear or so-called "π-pulse" regime, characterized by the self-similar contracting pulse envelope.[6] The asymptotic equivalence expressed by Eq. (10) suggests that asymptotically identical pulses in the linear regime should evolve to identical pulses in the nonlinear regime. In the limit of short (δ function) laser seeds, and correspondingly short plasma seeds, a formal equivalence can be made. While the finite width case does not follow rigorously, we show numerically that the equivalence in fact does extend to finite pulse widths.

The effects of finite seed width and finite plasma temperature are examined using one-dimensional PIC simulations and the simulation results are reported is reported in Ref.[7] The simulations take experimental feasible parameters:[30, 35] $n_e = 1.5 \times 10^{19} \mathrm{cm^{-3}}$, $T_e = 10\,\mathrm{eV}$, $\lambda_a = 0.8\,\mu\mathrm{m}$ and $I_a = 0.4\,\mathrm{PW\,cm^{-2}}$. The simulations compare amplifications of a Gaussian shape laser seed and a nearly equivalent plasma wave seed. The laser seed has a width of $10\,\mu\mathrm{m} \approx 0.16 c/\gamma_0$ and peak intensity of $0.8\,\mathrm{TW\,cm^{-2}}$. The plasma wave seed uses a single Gaussian profile to approximate the equivalence, with a normalized width $7.1\,\mu\mathrm{m} \approx 0.117\,c/\gamma_0$, while ignoring the second peak. The amplitude of the electrostatic seed wave is $5 \times 10^9\,\mathrm{V/m}$, which is associated with a 50% electron density oscillation. Its wavelength is $0.4\,\mu\mathrm{m}$, so that $k_p = 2k_a$.

Note that, immediately after the interaction, a probe beam is generated [see Fig. 4(a)]. The comparison indicates that the plasma seed indeed triggers the Raman amplification like a laser seed does. No precursors
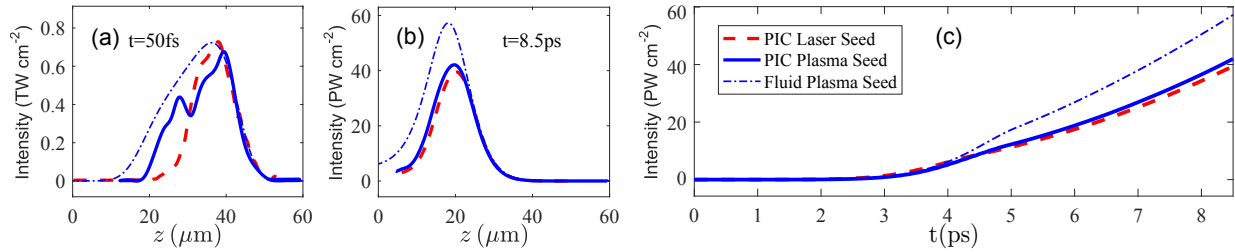
Figure 4. Amplified probe pulses using a plasma seed (blue solid line) and a laser seed (red dashed line) at interaction time $t = 50\,$fs (a) and $t = 8.5\,$ps (b). (c) Comparison of the amplified probe pulse peak intensity. The thick solid and dashed lines are PIC simulations; and the thin dotted-dash lines are fluid-model simulations using Eqs.(1). Adapted from *Qu, Barth and Fisch (2017)*,[7] with the permission of American Physical Society.

are observed, but the moving window would suppress those. In Fig. 4(c), which shows the growth of the peak intensity, we identify the linear stage amplification (before $\sim 4.5\,$ps), exhibiting an intensity exponentially increasing in time (or distance) and the nonlinear stage (after $\sim 4.5\,$ps), exhibiting a quadratically increasing intensity. After an amplification time of $8.5\,$ps, the leading spikes of the probes shown in Fig. 4(b) both reach $40\,\mathrm{PW\,cm^{-2}}$, which is 100 times higher than the pump intensity. The pump depletion at the probe peak is 75% for both seeds. The agreement between the PIC simulations with plasma and laser seeds is very good for both the leading peak envelopes [Fig. 4(b)] and the maximum intensity [Fig. 4(c)]. They also decently match the numerical solutions of Eq. (1), although PIC simulations show asymptotically lower peak intensities. The discrepancy might be due to kinetic effects that are taken into account in PIC, but not in the fluid model, or due to the envelope approximation in the fluid model.

For higher plasma density where GVD becomes important, one can advantageously chirp the laser seed to reduce the required plasma length.[64] Since higher frequency components propagate faster, the front of the chirped probe sharpens due to GVD. In fact, for plasma seeds, the advantageous chirping effects can be accomplished by chirping the wavelength of the plasma wave. When it scatters off the monochromatic pump, the generated probe is also chirped and hence can contract due to GVD.
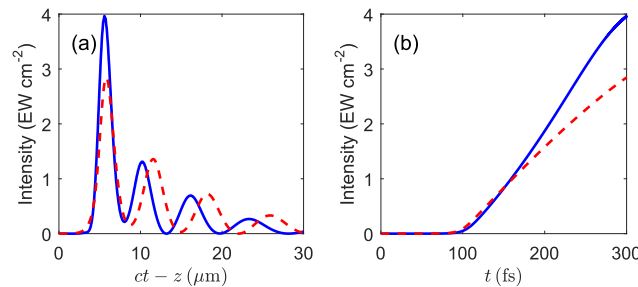

Figure 5. (a) Amplified probe beams triggered by chirped (blue solid) and non-chirped (red dashed) plasma seeds with a $600\,$fs pump pulse; (b) growth of the peak intensities. The seed amplitudes and shapes are identical. Reprinted from *Qu, Barth and Fisch (2017)*,[7] with the permission of American Physical Society.

The effect of chirping and GVD can be shown by numerically solving the first-order three-wave equations,[64]

$$a_t - ca_z = -Vbf, \quad b_t + cb_z = Vaf^* + i\kappa b_{tt}, \quad f_t = Vab^*, \tag{14}$$

which is obtained by reducing the three-wave Eqs.(1)-(3). Here, $\kappa = (1/2c_b)(\partial c_b/\partial \omega_b) = \omega_p^2/(2c_b\omega_b)$ and c_b is the group velocity of the seed. Figure 5 is reported in Ref.[7] to compare amplification in a high density plasma with a chirped plasma seed to amplification with a non-chirped plasma seed. The parameters are chosen similar to those in Ref.,[64] *i.e.*, $n_e = 12 \times 10^{20}\mathrm{cm^{-3}}$, $\lambda_a = 0.351\,\mu\mathrm{m}$, $I_a = 12.2\,\mathrm{PW\,cm^{-2}}$ and the plasma length is $90\,\mu\mathrm{m}$. The plasma seeds are both Gaussian with FWHM of $1.8\,\mu\mathrm{m}$. The nonchirped seed has a uniform wavevector $k_f = k_a + k_b = 2\pi/0.215\,\mu\mathrm{m}$. Its output intensity reaches $2.8\,\mathrm{EW\,cm^{-2}}$. Here, the wavevector, k_f, of the chirped plasma seed increased 3.5% per $\mu\mathrm{m}$, where pump interacts with lower k_f first. Since the pump has a constant

frequency, the generated probe is also chirped with smaller wavenumbers (smaller frequencies) at the front. Due to GVD, the probe contracts when traveling through the plasma. Similar to the case of a chirped laser seed,[64] the probe beam has a larger growth rate and its intensity reaches $4\,\mathrm{EW\,cm^{-2}}$. From Fig. 5(a), we also observe an appropriately narrower probe pulse.

The equivalence of plasma and laser seeds is limited by accessible amplitude of the plasma wave. While a seed laser pulse can take an arbitrarily large amplitude, the Langmuir wave seed amplitude will be limited by the wavebreaking limit. In a cold plasma, this condition is equivalent to a maximum density variation $\delta n < n_0$; in a warm plasma the density variation is somewhat more limited.[65,66] However, this will not be an issue in the main amplification regimes[67] for which the necessary laser seeding amplitudes can be small.[45] Also, even a small plasma wave seed can access operation near the wave breaking limit,[42,43] since that limit is determined by the pump amplitude, not the seed amplitude. The density restriction may be an issue though in the so-called *quasi-transient* regime, where damping of the Langmuir wave is significant, so amplification is achieved only with larger laser seed amplitudes.[68,69] The corresponding amplitudes may then not be available for plasma wave seeds. However, these regimes are in any event not of interest for plasma wave seeding, since, if the plasma wave is heavily damped, the advantage of synchronization is absent.

4. RAMAN AMPLIFICATION WITH PARTIALLY COHERENT PUMP LASERS

While the precursors of the seed can be eliminated by using an optical shutter or using localized plasma waves, plasma noise due to random density fluctuation can quickly grow in backward Raman amplification and lead to reflection of the laser and causes pre-mature pump depletion. To address the noise-seeded spontaneous Raman scattering, one is optimally looking for a solution that suppresses the linear growth Raman rate while maintains the nonlinear growth rate. To this end, it has been proposed[10] to replace the coherent pump laser with a laser whose coherence length is shorter than the Raman growth rate. Through analytical calculation and numerical simulations, Raman amplification with the partially coherent lasers is shown to efficiently compress a temporally incoherent pump laser into an intense coherent amplified seed pulse and suppress spontaneous noise amplification.

By solving the same model for Raman amplification [Eqs. (14)], the pulse amplification by an incoherent pump can be described by an integral equation in a moving frame ($\zeta = t - z/v_b$ and $\tau = z/v_b$),

$$b(\zeta,0) = b(\zeta,\tau) - \int_0^\zeta \Gamma^2 g(2\zeta - 2\zeta')e^{\nu(\zeta'-\zeta)} \int_0^\tau b(\zeta',\tau')\mathrm{d}\tau'\mathrm{d}\zeta', \tag{15}$$

where $\Gamma = \langle a\rangle V$, $\langle a\rangle = \sqrt{\langle|a|^2\rangle}$ and $g(\Delta t) = \langle a^*(t-\Delta t)a(t)\rangle \big/ \langle|a(t)|^2\rangle$ is the correlation function of the pump beam. Here, we describe the effect of plasma wave damping with the damping rate ν. The integral Eq. (15) shows that an incoherent pump beam can amplify a coherent seed if the pump has a non-zero correlation length. The plasma wave damping term multiplies the autocorrelation function in the integral kernel; incoherence and plasma wave damping therefore have a similar effect on seed amplification. The analogy in the underlying physics arises because the plasma wave produced by the beating of the pump and seed drifts out of phase with the pump over the coherence time of the pump, leading to destructive interference and no net interaction beyond the pump coherence length. Similarly, damping of the plasma wave leaves no wave to interact with beyond the damping time.

The linear growth rate is affected by the pump incoherence and plasma wave damping. As an example of an exponentially decreasing autocorrelation function $g(\zeta) = e^{-\zeta/t_c}$, the effective growth rate is[10]

$$\bar{\Gamma} = \frac{\Gamma^2}{(\nu + 2/t_c) + \sqrt{\Gamma^2 + (\nu + 2/t_c)^2}}, \tag{16}$$

and the seed maximum locates at

$$\zeta_M = \frac{ct}{2}\left(1 - \sqrt{\frac{(\nu + 2/t_c)^2}{1 + (\nu + 2/t_c)^2}}\right). \tag{17}$$

In the limit of no damping and a fully coherent pump, the plasma wave, once generated, scatters the pump continuously, producing a monotonically growing wavefront along ζ. For damping and a finite correlation length,
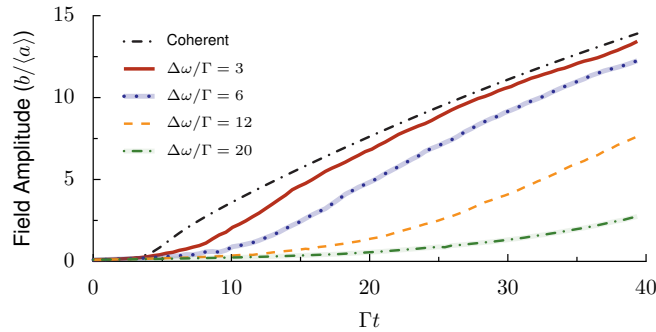
Figure 6. Maximum field strength of the seed as a function of amplification time for different degrees of pump incoherence from a three-wave simulation of the amplification process. The seed amplitude is normalized by the pump amplitude. Reprinted from *Edwards, Qu, Mikhailova and Fisch (2017),*[10] with the permission of AIP Publishing.

the plasma wave scatters the pump only for a finite amount of time and then the interaction stops. This reduces the growth rate at the seed tail, hence the pulse maximum shifts towards the front and the peak growth rate is reduced. The effect of pump incoherence is similar to the *quasi-transient* regime[69] of Raman amplification, in which the plasma wave quickly damps causing the interaction to exist only near the strong seed pulse.

The seed growth rate in the nonlinear stage can, however, tolerate more pump incoherence. In the nonlinear stage, the strong seed depletes the pump energy; the front of the seed is preferentially amplified causing seed duration compression. The compression of the amplified pulses shortens the time over which the pump must retain its coherence with the plasma wave in order for the interaction to be treated as coherent. The key time for determining whether incoherence hinders the amplification process then becomes the duration of the final amplified pulse. Since the pulse duration can reach the order of the inverse plasma frequency (ω_p), which may be several orders of magnitude shorter than the inverse Raman growth time, the regime of efficient nonlinear amplification is much broader than that of linear amplification.

Comparison of the seed growth in the linear and nonlinear regimes under different degrees of pump incoherence has been shown in Ref.[43] By numerically solving the coupled wave Eqs. (14), the results displayed in Fig. 6 show the evolution of the maximum seed intensity. In the linear stage when the relative seed amplitude is below ~ 2.5, one can readily see the reduced growth rate with a larger degree of pump incoherence. However, when the seed is sufficiently strong to enter the nonlinear stage, their leading spikes growth rates are almost independent of the degree of pump incoherence, even for $\Delta\omega/\Gamma > 12$. The different final intensities in this figure are almost entirely a result of the much lower linear growth rate for incoherent pumps.
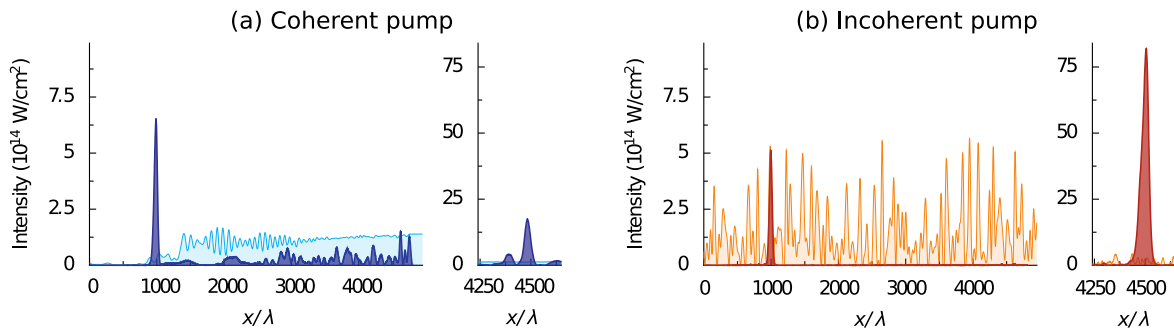

Figure 7. One-dimensional PIC simulations (EPOCH) with coherent (a) and incoherent (b) pumps showing amplification of a seed (blue, red). In (a), the pump spontaneously scatters from noise, causing pre-depletion of the pump before arrival of the seed and reducing amplification efficiency. At right, the final amplified pulse is much stronger when using an incoherent pump, due to the reduced loss of pump energy. $N = 0.01$, $a_0 = 0.01$, and $T_e = 25$ eV. For (b), $\Delta\omega/\omega = 0.04$. The simulations used 40 particles/cell and 40 cells/λ. The initial seed had duration 50 T_L and maximum intensity equal to the average pump intensity. $\lambda = 1$ μm. Adapted from *Edwards, Qu, Mikhailova and Fisch (2017),*[10] with the permission of AIP Publishing.

The discrepancy in the linear and nonlinear growth rate using partially coherent laser is used to suppress unwanted seed precursors and parasitic noise-seeded Raman scattering. Starting with a sufficiently strong laser seed, the Raman amplification can directly reach the nonlinear stage and efficiently capture the pump energy. However, amplification of the low-amplitude noise is significantly suppressed by the reduced linear growth rate. The suppression of noise is even more effective than the fluid model can predict because the frequency fluctuation of noise can cause a phase mismatch which further reduces the growth rate. The PIC simulation results reported in Ref.[10] have demonstrated the advantage of using partially coherent pump in a proposed experiment. In Fig. 7(a), noise-seeded spontaneous Raman backscattering will grow at the effective Raman growth rate $\bar{\Gamma}$, as given for a pump with exponentially decreasing coherence by Eq. (16). However, the amplification of a short, strong seed is not affected by the finite bandwidth. In Fig. 7(a), a significant fraction of the pump is depleted by spontaneous Raman scattering before it has a chance to interact with the seed, leading to a loss of energy and the formation of substantial precursors before the seed. In Fig. 7(b), the finite bandwidth of the pump ($\Delta\omega/\omega_0 = 0.04$) suppresses premature noise scattering. In this case, the final amplified seed is almost four times more intense in the incoherent-pump case; amplification with an incoherent pump is more efficient than with a coherent pump.

5. CONCLUSION

This paper reviews the theoretical advances on using plasma optics to increase the efficiency of backward Raman amplification. We identify the technological challenges of creating the suitable seeds that can effectively compress the pump laser pulse and generate ultra high output intensity. Three plasma optics methods are made available to address the challenges. First, we design a high speed optical shutter in over-dense plasmas that can create a sharp wavefront to a seed laser beam. The optical shutter is controlled by a separate laser beam at a different frequency. When the control laser beam exceeds a threshold intensity, it abruptly induces a transparency window in the over-dense plasma, leading to a sharp transmission wavefront in the seed beam. Unlike plasma mirrors[70–72] or relativistic transparency,[60] the control beam does not need to reach relativistic intensity and the seed beam does not lose energy.

Second, we show that one can replace the traditional laser seed pulse by a plasma wave seed with a certain envelope in backward Raman amplification. An equivalence condition is found to use a plasma wave seed to produce the same output pulse in the asymptotic pump-depletion regime as does a counter-propagating laser seed. A localized static plasma wave seed avoids the technological challenges regarding alignment, downshifting the laser pulse frequency and eliminate pre-pulses.

Third, we show how an partially incoherent pump laser can suppress the noise-induced spontaneous Raman amplification and yield higher output intensity than fully coherent pump lasers do. Noise suppression using incoherent pump arises from the discrepancy that the stronger seed can tolerate more pump incoherence. For Raman scattering of noise or low-energy pre-pulses, the Raman growth rate is low because they only interact with a small portion of pump spectrum that is on resonance. But a strong seed pulse has a wide spectrum and it can efficiently capture a larger pump spectrum and hence it is more tolerant to pump incoherence.

REFERENCES

[1] Stuart, B. C., Feit, M. D., Rubenchik, A. M., Shore, B. W., and Perry, M. D., "Laser-induced damage in dielectrics with nanosecond to subpicosecond pulses," *Phys. Rev. Lett.* **74**, 2248 (1995).

[2] Canova, F., Uteza, O., Chambaret, J.-P., Flury, M., Tonchev, S., Fechner, R., and Parriaux, O., "High-efficiency, broad band, high-damage threshold high-index gratings for femtosecond pulse compression," *Opt. Express* **15**, 15324 (2007).

[3] Nicola, J. D., Bond, T., Bowers, M., Chang, L., Hermann, M., House, R., Lewis, T., Manes, K., Mennerat, G., MacGowan, B., Negres, R., Olejniczak, B., Orth, C., Parham, T., Rana, S., Raymond, B., Rever, M., Schrauth, S., Shaw, M., Spaeth, M., Wonterghem, B. V., Williams, W., Widmayer, C., Yang, S., Whitman, P., and Wegner, P., "The national ignition facility: laser performance status and performance quad results at elevated energy," *Nucl. Fusion* **59**, 032004 (2018).

[4] Strickland, D. and Mourou, G., "Compression of amplified chirped optical pulses," *Opt. Commun.* **55**, 447 (1985).

[5] Shvets, G., Fisch, N. J., Pukhov, A., and Meyer-ter-Vehn, J., "Superradiant amplification of an ultrashort laser pulse in a plasma by a counterpropagating pump," *Phys. Rev. Lett.* **81**, 4879 (1998).

[6] Malkin, V. M., Shvets, G., and Fisch, N. J., "Fast compression of laser beams to highly overcritical powers," *Phys. Rev. Lett.* **82**, 4448 (1999).

[7] Qu, K., Barth, I., and Fisch, N. J., "Plasma wave seed for Raman amplifiers," *Phys. Rev. Lett.* **118**, 164801 (2017).

[8] Qu, K. and Fisch, N. J., "Laser pulse sharpening with electromagnetically induced transparency in plasma," *Phys. Plasmas* **24**, 073108 (2017).

[9] Kirkwood, R. K., Turnbull, D. P., Chapman, T., Wilks, S. C., Rosen, M. D., London, R. A., Pickworth, L. A., Dunlop, W. H., Moody, J. D., Strozzi, D. J., Michel, P. A., Divol, L., Landen, O. L., MacGowan, B. J., Van Wonterghem, B. M., Fournier, K. B., and Blue, B. E., "Plasma-based beam combiner for very high fluence and energy," *Nat. Phys.* **14**, 80 (2017).

[10] Edwards, M. R., Qu, K., Mikhailova, J. M., and Fisch, N. J., "Beam cleaning of an incoherent laser via plasma Raman amplification," *Phys. Plasmas* **24**, 103110 (2017).

[11] Michel, P., Divol, L., Turnbull, D., and Moody, J. D., "Dynamic control of the polarization of intense laser beams via optical wave mixing in plasmas," *Phys. Rev. Lett.* **113**, 205001 (2014).

[12] Turnbull, D., Michel, P., Chapman, T., Tubman, E., Pollock, B. B., Chen, C. Y., Goyon, C., Ross, J. S., Divol, L., Woolsey, N., and Moody, J. D., "High power dynamic polarization control using plasma photonics," *Phys. Rev. Lett.* **116**, 205001 (2016).

[13] Lehmann, G. and Spatschek, K. H., "Plasma-based polarizer and waveplate at large laser intensity," *Phys. Rev. E* **97**, 063201 (2018).

[14] Zhang, X., Shen, B., Shi, Y., Wang, X., Zhang, L., Wang, W., Xu, J., Yi, L., and Xu, Z., "Generation of intense high-order vortex harmonics," *Phys. Rev. Lett.* **114**, 173901 (2015).

[15] Vieira, J., Trines, R. M. G. M., Alves, E. P., Fonseca, R. A., Mendonça, J. T., Bingham, R., Norreys, P., and Silva, L. O., "High orbital angular momentum harmonic generation," *Phys. Rev. Lett.* **117**, 265001 (2016).

[16] Vieira, J., Trines, R. M. G. M., Alves, E. P., Fonseca, R. A., Mendonça, J. T., Bingham, R., Norreys, P., and Silva, L. O., "Amplification and generation of ultra-intense twisted laser pulses via stimulated Raman scattering," *Nat. Commun.* **7**, 10371 (2016).

[17] Leblanc, A., Denoeud, A., Chopineau, L., Mennerat, G., Martin, P., and Quéré, F., "Plasma holograms for ultrahigh-intensity optics," *Nat. Phys.* **13**, 440 (2017).

[18] Qu, K., Jia, Q., and Fisch, N. J., "Plasma *q*-plate for generation and manipulation of intense optical vortices," *Phys. Rev. E* **96**, 053207 (2017).

[19] Monchocé, S., Kahaly, S., Leblanc, A., Videau, L., Combis, P., Réau, F., Garzella, D., D'Oliveira, P., Martin, P., and Quéré, F., "Optically controlled solid-density transient plasma gratings," *Phys. Rev. Lett.* **112**, 145008 (2014).

[20] Lehmann, G. and Spatschek, K. H., "Transient plasma photonic crystals for high-power lasers," *Phys. Rev. Lett.* **116**, 225002 (2016).

[21] Lehmann, G. and Spatschek, K. H., "Laser-driven plasma photonic crystals for high-power lasers," *Phys. Plasmas* **24**, 056701 (2017).

[22] Shen, K. F. and Guo, B., "Realization of tunable TE/TM wave splitter with one-dimensional plasma dielectric photonic crystal," *Int. J. Mod. Phys. B* **32**, 1850253 (2018).

[23] Dodin, I. Y. and Fisch, N. J., "Storing, retrieving, and processing optical information by Raman backscattering in plasmas," *Phys. Rev. Lett.* **88**, 165001 (2002).

[24] Edwards, M. R., Qu, K., Jia, Q., Mikhailova, J. M., and Fisch, N. J., "Cascaded chirped photon acceleration for efficient frequency conversion," *Phys. Plasmas* **25**, 053102 (2018).

[25] Qu, K., Jia, Q., Edwards, M. R., and Fisch, N. J., "Theory of electromagnetic wave frequency upconversion in dynamic media," *Phys. Rev. E* **98**, 023202 (2018).

[26] Malkin, V., Shvets, G., and Fisch, N., "Detuned Raman amplification of short laser pulses in plasma," *Phys. Rev. Lett.* **84**, 1208 (2000).

[27] Malkin, V. M., Shvets, G., and Fisch, N. J., "Ultra-powerful compact amplifiers for short laser pulses," *Phys. Plasmas* **7**, 2232 (2000).

[28] Ping, Y., Geltner, I., Fisch, N., Shvets, G., and Suckewer, S., "Demonstration of ultrashort laser pulse amplification in plasmas by a counterpropagating pumping beam," *Phys. Rev. E* **62**, R4532 (2000).

[29] Dreher, M., Takahashi, E., Meyer-ter-Vehn, J., and Witte, K.-J., "Observation of superradiant amplification of ultrashort laser pulses in a plasma," *Phys. Rev. Lett.* **93**, 095001 (2004).

[30] Cheng, W., Avitzour, Y., Ping, Y., Suckewer, S., Fisch, N. J., Hur, M. S., and Wurtele, J. S., "Reaching the nonlinear regime of Raman amplification of ultrashort laser pulses," *Phys. Rev. Lett.* **94**, 045003 (2005).

[31] Ren, J., Cheng, W., Li, S., and Suckewer, S., "A new method for generating ultraintense and ultrashort laser pulses," *Nat. Phys.* **3**, 732 (2007).

[32] Ping, Y., Cheng, W., Suckewer, S., Clark, D. S., and Fisch, N. J., "Amplification of ultrashort laser pulses by a resonant Raman scheme in a gas-jet plasma," *Phys. Rev. Lett.* **92**, 175007 (2004).

[33] Kirkwood, R., Dewald, E., Niemann, C., Meezan, N., Wilks, S., Price, D., Landen, O., Wurtele, J., Charman, A., Lindberg, R., Fisch, N., Malkin, V., and Valeo, E., "Amplification of an ultrashort pulse laser by stimulated Raman scattering of a 1ns pulse in a low density plasma," *Phys. Plasmas* **14**, 113109 (2007).

[34] Ren, J., Li, S., Morozov, A., Suckewer, S., Yampolsky, N., Malkin, V., and Fisch, N., "A compact double-pass Raman backscattering amplifier/compressor," *Phys. Plasmas* **15**, 056702 (2008).

[35] Ping, Y., Kirkwood, R., Wang, T.-L., Clark, D., Wilks, S., Meezan, N., Berger, R., Wurtele, J., Fisch, N., Malkin, V., et al., "Development of a nanosecond-laser-pumped Raman amplifier for short laser pulses in plasma," *Phys. Plasmas* **16**, 123113 (2009).

[36] Turnbull, D., Li, S., Morozov, A., and Suckewer, S., "Possible origins of a time-resolved frequency shift in Raman plasma amplifiers," *Phys. Plasmas* **19**, 073103 (2012).

[37] Depierreux, S., Yahia, V., Goyon, C., Loisel, G., Masson-Laborde, P. E., Borisenko, N., Orekhov, A., Rosmej, O., Rienecker, T., and Labaune, C., "Laser light triggers increased Raman amplification in the regime of nonlinear Landau damping," *Nat. Commun.* **5**, 4158 (2014).

[38] Vieux, G., Cipiccia, S., Grant, D. W., Lemos, N., Grant, P., Ciocarlan, C., Ersfeld, B., Hur, M. S., Lepipas, P., Manahan, G. G., Raj, G., Reboredo Gil, D., Subiel, A., Welsh, G. H., Wiggins, S. M., Yoffe, S. R., Farmer, J. P., Aniculaesei, C., Brunetti, E., Yang, X., Heathcote, R., Nersisyan, G., Lewis, C. L. S., Pukhov, A., Dias, J. M., and Jaroszynski, D. A., "An ultra-high gain and efficient amplifier based on Raman amplification in plasma," *Sci. Rep.* **7**, 2399 (2017).

[39] Ping, Y., Geltner, I., Morozov, A., Fisch, N., and Suckewer, S., "Raman amplification of ultrashort laser pulses in microcapillary plasmas," *Phys. Rev. E* **66**, 046401 (2002).

[40] Pai, C.-H., Lin, M.-W., Ha, L.-C., Huang, S.-T., Tsou, Y.-C., Chu, H.-H., Lin, J.-Y., Wang, J., and Chen, S.-Y., "Backward Raman amplification in a plasma waveguide," *Phys. Rev. Lett.* **101**, 065005 (2008).

[41] Yampolsky, N. A. and Fisch, N. J., "Limiting effects on laser compression by resonant backward Raman scattering in modern experiments," *Phys. Plasmas* **18**, 056711 (2011).

[42] Toroker, Z., Malkin, V. M., and Fisch, N. J., "Backward Raman amplification in the Langmuir wavebreaking regime," *Phys. Plasmas* **21**, 113110 (2014).

[43] Edwards, M. R., Toroker, Z., Mikhailova, J. M., and Fisch, N. J., "The efficiency of Raman amplification in the wavebreaking regime," *Phys. Plasmas* **22**, 074501 (2015).

[44] Tsidulko, Y. A., Malkin, V. M., and Fisch, N. J., "Suppression of superluminous precursors in high-power backward Raman amplifiers," *Phys. Rev. Lett.* **88**, 235004 (2002).

[45] Yampolsky, N. A., Malkin, V. M., and Fisch, N. J., "Finite-duration seeding effects in powerful backward Raman amplifiers," *Phys. Rev. E* **69**, 036401 (2004).

[46] Yampolsky, N., Fisch, N., Malkin, V., Valeo, E., Lindberg, R., Wurtele, J., Ren, J., Li, S., Morozov, A., and Suckewer, S., "Demonstration of detuning and wavebreaking effects on Raman amplification efficiency in plasma," *Phys. Plasmas* **15**, 113104 (2008).

[47] Balakin, A. A., Fraiman, G. M., Fisch, N. J., and Malkin, V. M., "Noise suppression and enhanced focusability in plasma Raman amplifier with multi-frequency pump," *Phys. Plasmas* **10**, 4856 (2003).

[48] Malkin, V. M. and Fisch, N. J., "Key plasma parameters for resonant backward Raman amplification in plasma," *Eur. Phys. J. Spec. Top.* **223**, 1157 (2014).

[49] Cole, B., Goldberg, L., Trussell, C. W., Hays, A., Schilling, B. W., and McIntosh, C., "Reduction of timing jitter in a Q-switched Nd:YAG laser by direct bleaching of a Cr4+:YAG saturable absorber," *Opt. Express* **17**, 1766 (2009).

[50] Fourmaux, S., Payeur, S., Buffechoux, S., Lassonde, P., St-Pierre, C., Martin, F., and Kieffer, J. C., "Pedestal cleaning for high laser pulse contrast ratio with a 100 TW class laser system," *Opt. Express* **19**, 8486 (2011).

[51] Keppler, S., Sävert, A., Körner, J., Hornung, M., Liebetrau, H., Hein, J., and Kaluza, M. C., "The generation of amplified spontaneous emission in high-power CPA laser systems," *Laser Photonics Rev.* **10**, 264 (2016).

[52] Haus, H. A. and Mecozzi, A., "Noise of mode-locked lasers," *IEEE J. Quantum Electron.* **29**, 983 (1993).

[53] Keller, U., "Recent developments in compact ultrafast lasers," *Nature* **424**, 831 (2003).

[54] Harris, S. E., "Electromagnetically induced transparency in an ideal plasma," *Phys. Rev. Lett.* **77**, 5357 (1996).

[55] Marangos, J. P., "Electromagnetically induced transparency," *J. Mod. Opt.* **45**, 471 (1998).

[56] Matsko, A. B. and Rostovtsev, Y. V., "Electromagnetic-wave propagation and amplification in overdense plasmas: Application to free electron lasers," *Phys. Rev. E* **58**, 7846 (1998).

[57] Gordon, D. F., Mori, W. B., and Joshi, C., "On the possibility of electromagnetically induced transparency in a plasma. I. infinite plasma," *Phys. Plasmas* **7**, 3145 (2000).

[58] Gordon, D. F., Mori, W. B., and Joshi, C., "On the possibility of electromagnetically induced transparency in a plasma. II. bounded plasma," *Phys. Plasmas* **7**, 3156 (2000).

[59] Ersfeld, B. and Jaroszynski, D. A., "Electromagnetically induced transparency for two intense waves in plasma," *J. Mod. Opt.* **49**, 889 (2002).

[60] Palaniyappan, S., Hegelich, B. M., Wu, H.-C., Jung, D., Gautier, D. C., Yin, L., Albright, B. J., Johnson, R. P., Shimada, T., Letzring, S., Offermann, D. T., Ren, J., Huang, C., Horlein, R., Dromey, B., Fernandez, J. C., and Shah, R. C., "Dynamics of relativistic transparency and optical shuttering in expanding overdense plasmas," *Nat. Phys.* **8**, 763 (2012).

[61] Arber, T. D., Bennett, K., Brady, C. S., Lawrence-Douglas, A., Ramsay, M. G., Sircombe, N. J., Gillies, P., Evans, R. G., Schmitz, H., Bell, A. R., et al., "Contemporary particle-in-cell approach to laser-plasma modelling," *Plasma Phy. Contr. F.* **57**, 113001 (2015).

[62] Forslund, D. W., Kindel, J. M., and Lindman, E. L., "Theory of stimulated scattering processes in laser-irradiated plasmas," *Phys. Fluids* **18**, 1002 (1975).

[63] Shvets, G. and Wurtele, J. S., "Free electron lasers 1996 SASE in plasmas: Analysis and simulation of Raman backscatter from noise," *Nucl. Instrum. Meth. A* **393**, 371 (1997).

[64] Toroker, Z., Malkin, V., and Fisch, N., "Seed laser chirping for enhanced backward Raman amplification in plasmas," *Phys. Rev. Lett.* **109**, 085003 (2012).

[65] Coffey, T. P., "Breaking of large amplitude plasma oscillations," *Phys. Fluids* **14**, 1402 (1971).

[66] Bergmann, A. and Schnabl, H., "The influence of electron trapping on stationary Langmuir waves," *Phys. Plasmas* **31**, 3266 (1988).

[67] Clark, D. S. and Fisch, N. J., "Operating regime for a backward Raman laser amplifier in preformed plasma," *Phys. Plasmas* **8**, 3363 (2003).

[68] Malkin, V. M. and Fisch, N. J., "Quasitransient regimes of backward Raman amplification of intense X-ray pulses," *Phys. Rev. E* **80**, 046409 (2009).

[69] Malkin, V. M. and Fisch, N. J., "Quasitransient backward Raman amplification of powerful laser pulses in dense plasmas with multicharged ions," *Phys. Plasmas* **17**, 073109 (2010).

[70] Thaury, C., Quéré, F., Geindre, J.-P., Levy, A., Ceccotti, T., Monot, P., Bougeard, M., Réau, F., dOliveira, P., Audebert, P., et al., "Plasma mirrors for ultrahigh-intensity optics," *Nat. Phys.* **3**, 424 (2007).

[71] Doumy, G., Quéré, F., Gobert, O., Perdrix, M., Martin, P., Audebert, P., Gauthier, J., Geindre, J.-P., and Wittmann, T., "Complete characterization of a plasma mirror for the production of high-contrast ultraintense laser pulses," *Phys. Rev. E* **69**, 026402 (2004).

[72] Mikhailova, J. M., Buck, A., Borot, A., Schmid, K., Sears, C., Tsakiris, G. D., Krausz, F., and Veisz, L., "Ultra-high-contrast few-cycle pulses for multipetawatt-class laser technology," *Opt. Lett.* **36**, 3145 (2011).